Classical and Quantum Description of the Kapitza-Dirac Effect

Darius-Matei Banu[1†], Richard Radu[1†], Madalina Boca[1*†]

[1*]Department of Physics, University of Bucharest, Atomistilor 405, Magurele, 077125, lfov, Romania.

*Corresponding author(s). E-mail(s): madalina.boca@unibuc.ro;
Contributing authors: darius-matei.banu@s.unibuc.ro;
richard-andrei.radu@s.unibuc.ro;
†These authors contributed equally to this work.

Abstract

In this work we explore the classical and quantum descriptions of the Kapitza-Dirac effect, the scattering of charged particles by a standing wave electromagnetic field. In the classical case, initially we integrate numerically the covariant Lorentz force equation, for a statistical ensemble of electrons interacting with a superposition of two linearly polarized plane waves. We then employ the relativistic ponderomotive force approximation to the same initial conditions, and compare the two approaches across different field intensities. We present a graphical representation of the final momentum's distribution as a function of the particles' initial positions for different field intensities and scattering geometries, and we study the dependence of the magnitude of the momentum transfer on the field intensity. In the quantum case we consider the Klein-Gordon equation for a charged particle interacting with the same elecromagentic field. We look for a solution of a particular form, inspired by the well known Klein-Gordon Volkov states, and we show that in this case the Klein-Gordon equation reduces to a linear Goursat equation, which we solve numerically. The exact quantum results are compared both with the classical predictions and with an analytical approximation. We find that, in the intensity domain considered, the quantum and classical approximations are in agreement.

Keywords: Kapitza-Dirac effect, ponderomotive approximation, Klein-Gordon equation, Goursat problem

PAC Codes: 34.80.Qb , 41.75.Ht , 03.65.Pm , 45.10.-b

1 Introduction

The study of the time evolution of an electron in a crossed plane wave electromagnetic field has been a subject of interest for many years. The classical treatment, based on the solving of the relativistic or non relativistic Lorentz force equations, constitutes a very good model for testing different variants of the ponderomotive force approximation [1–4], or for studying the transition from the regular to chaotic motion of the particles [5]. An important characteristic of the process is that, if the two plane waves have different propagation directions, the momentum transfer is possible: the electron's final momentum differs from its initial value. By contrast, in the case of a single plane wave the equation of motion can be solved analytically [6], and one can prove that for any initial conditions the velocity of the particle at the end of the interaction is the same as at the initial moment. Our analysis focuses on the momentum transfer, and on its dependence on the initial conditions and the field parameters. We also test the validity of the ponderomotive approximation over a range of field intensities.

The quantum treatment is based on solving of the Klein-Gordon equation, which is simpler than the Dirac equation, and generally yields results equivalent to those of the Dirac equation when spin effects are negligible. On the other hand, we emphasize here that the general techniques developed for the solution of the Klein-Gordon equation can be easily extended also for the Dirac equation. Similar to the classical case, both the Klein-Gordon and the Dirac equation admit an analytical solution for the case of a single plane wave; the solutions are the so called Volkov states [7–9]; interestingly, the Volkov solutions of the Schrödinger equation can not be derived in analytical form. The interest in the study of the solutions of the Dirac/Klein Gordon equation in a superposition of two plane waves is given, on the one hand, on the fact that they are the basis of the theoretical study of the Kapitza-Dirac effect [10], which is the diffraction of particles on a standing wave electromagnetic field (see also [11, 12]). On the other hand, the study of exact quantum relativistic solutions for an electron in crossed laser beams could provide a powerful tool for studying pair production in intense fields [13], or for quantum treatment of radiation reaction [14, 15].

A paper by Gavrila [16] presents approximate analytical solutions for the Klein-Gordon equation in an arbitrary superposition of plane waves. It also discusses the time evolution of an arbitrary wavepacket in the presence of such a field. The general result of Gavrila's paper is that, within the approximation used, the momentum distribution of the wavepacket at the end of the interaction is the same as the momentum distribution of the wavepacket at the initial moment, i.e., again, the net momentum transfer is zero. Using the approach of Gavrila as the starting point we derive a numerical method for solving the Klein-Gordon equation in the case of two plane waves; as we explain in Sect. 2, the method is valid for arbitrary geometry and polarization, and also for arbitrary initial conditions, being at the same time relatively easy to implement and inexpensive in computational time.

The paper is structured as follows: in the next section we present elements of theory: we define the electromagnetic field used in the calculations, we present briefly the covariant Lorentz force equations, and the ponderomotive force approximation. We also present, in the quantum framework, the Klein-Gordon equation and the derivation of a Goursat problem equivalent to it. In the third section we present the

numerical results for the classical and quantum cases, and, finally, in the fourth section we present our conclusions. The paper has also two appendices: in the first appendix we present the relativistic equations of motion for a free particle of variable mass, and in the second appendix we briefly review the main properties the Volkov solutions of the Klein-Gordon equation.

In the derivation of the theoretical equations we use the International System of Units (SI); our numerical results are presented in atomic units. The Minkowski metric used through the text is $(+,-,-,-)$.

2 Elements of theory

2.1 The electromagnetic field and the covariant Lorentz force equations

We consider a plane wave electromagnetic field, propagating along the unit vector $\mathbf{n}$; in this case, it is convenient to introduce a 4-vector of zero norm

$$n = (1, \mathbf{n}). \tag{1}$$

The four-wave vector k will be then given by

$$k = \frac{\omega}{c} n. \tag{2}$$

with ω the central frequency of the field. The electromagnetic field propagating in vacuum can be described by the four-vector potential

$$A(x) = A_0 f(k \cdot x) \mathrm{Re}\left\{\epsilon e^{ik\cdot x}\right\} \tag{3}$$

where A_0 is the amplitude of the field. It is convenient to characterize the field intensity by the dimensionless parameter

$$\xi_0 = \frac{|e| A_0}{m_0 c} \tag{4}$$

where e_0, m_0 are the charge and mass of the electron. In the above expression x is the four-position, $x \equiv (ct, \mathbf{x})$, A_0 is the amplitude of the vector potential, ϵ is a constant polarization vector and k is the four-wave vector In the Lorentz gauge, the electromagnetic field obeys the equation $\partial \cdot A = 0$, which is equivalent to the condition that the four-vector potential is transverse, $k \cdot \epsilon = 0$. The function $f(k \cdot x)$ is a slowly varying envelope of the field, usually taken as a Gaussian function, and its role is to make the plane wave field of finite duration

$$A(k \cdot x) \approxeq 0 \quad \mathrm{i}f \quad \phi_m \leq k \cdot x \leq \phi_M, \tag{5}$$

.

In our problem, we consider a superposition of two linearly polarized plane waves,

$$A_i(x) = A_{0i} f(k_i \cdot x) \mathrm{Re}\left\{\epsilon_i e^{\mathrm{i}k_i \cdot x}\right\}, \qquad 1,2; \tag{6}$$

it is worth noting that the polarization 4-vectors ϵ_i are not unique, a transformation of the form $\epsilon_i \to \epsilon_i + \lambda k_i$ is equivalent to a gauge transformation and does not change the electromagnetic field. Using this property, we can arrange the polarization vectors such that each of them is orthogonal on both four-wave vectors

$$\epsilon_i \cdot k_j = 0, \qquad i,j = 1,2. \tag{7}$$

For example, starting with a polarization vector ϵ_1, non-orthogonal on k_2, we can perform the gauge transformation

$$\epsilon_1 \to \epsilon_1 + \lambda k_1, \qquad \lambda = -\frac{\epsilon_1 \cdot k_2}{k_2 \cdot k_2}. \tag{8}$$

and the new polarization vector will be orthogonal on both k_1 and k_2. As we shall see, this will simplify the calculations in the quantum case. For the following calculations it is convenient to introduce the notation $k_i \cdot x = \phi_i$, $i = 1,2$, and the vector potential (and also the fields) of a plane wave can be written as functions of a single variable ϕ_i

$$A_i(x) \to A_i(\phi_i) = \mathrm{Re}\left\{\epsilon_i a_i(\phi_i)\right\}, \qquad a_i(\phi_i) = A_0 f(\phi_i) e^{i\phi_i} \tag{9}$$

With these notations, the Faraday tensor of the plane wave will be

$$F_i^{\mu\nu} = \partial^\mu A_i^\nu - \partial^\nu A_i^\mu = a_i'(\phi_i)\left(k^\mu \epsilon_i^\nu - k^\nu \epsilon_i^\mu\right) \tag{10}$$

The equation of motion for a charged particle of mass m_0 and charge e_0 in the presence of the electromagnetic field is given by the covariant Lorentz force equations

$$\frac{dx^\mu}{d\tau} = u^\mu, \qquad \frac{du^\mu}{d\tau} = \frac{e_0}{m_0}\left(F_1^{\mu\nu} + F_2^{\mu\nu}\right) u_\nu \tag{11}$$

where τ is the proper time.

2.2 The ponderomotive force approximation

The ponderomotive force approximation applies to the motion of a particle in the presence of an electromagnetic field which presents a fast oscillation, modulated by a slowly varying envelope. The approximation averages out the fast oscillations of the Lagrangian, such that only the slow motion of the oscillations center is left. There are several ways to derive the relativistic version of the ponderomotive force approximation, see, for example [3, 5, 17]. Within the relativistic ponderomotive force approximation, the problem is reduced to the problem of the motion of a free particle, whose *mass is variable*; the variable mass is called the *dressed mass* and is given

by the expression

$$\mathcal{M}(x) = m\sqrt{1+a(x)}, \qquad a(x) = -\frac{e^2}{m^2c^2}\overline{A_\mu(x)A^\mu(x)}. \tag{12}$$

where the overline indicates the average over the fast oscillations of the electromagnetic field

$$\bar{f}(\mathrm{x},t) = \frac{1}{T}\int_{t-T/2}^{t+T/2} f\left(\mathrm{x},t'\right)dt'; \tag{13}$$

for simplicity in this paper we will consider only the case when both fields have the same frequency $\omega = \frac{2\pi}{T}$. The sign $-$ in form of the time average in Eq. (12) is due to the metric used $(+,-,-,-)$. For a more detailed presentation of the concept of electron dressing by the electromagnetic field within the quantum formalism see, for example [18]. The Lagrange equations for a particle of variable mass are derived in the appendix A; here we present briefly some details of the numerical calculation of the dressed mass and of its derivatives. By direct calculation we can easily see that the function $a(x)$ defined in (12) can be written as

$$a(x) = -\frac{e^2}{(mc)^2}\frac{1}{cT}\int_{-cT/2}^{cT/2} d\chi A_\alpha(x+\chi v)A^\alpha(x+\chi v), \qquad v \equiv (1,0,0,0), \tag{14}$$

and the integral can be calculated numerically using a quadrature method. Since the integrand is smooth enough function on the integration domain, which is of length $\lambda = cT$, the integration is inexpensive and can be done with good precision. For the Lagrange equations we also need the derivative of the dressed mass with respect to the coordinates and the velocities; by direct calculation we can easily see that

$$\partial^\mu\mathcal{M}(x) = m\partial^\mu\sqrt{1+a(x)} = \frac{m}{2}\partial^\mu a(x)\frac{1}{\sqrt{1+a(x)}} \tag{15}$$

and

$$\partial^\mu a(x) = -\frac{2e^2}{(mc)^2}\frac{1}{\lambda}\int_{-\lambda/2}^{\lambda/2} d\chi A_\alpha(x+\chi v)\cdot\partial^\mu A^\alpha(x+\chi v). \tag{16}$$

We can see that, because our field is a superposition of plane waves, even if the dressed mass itself is calculated as a numerical integral, its derivatives can be obtained by analytical derivation of the integrand, and again, only a numerical integration is required.

2.3 The Klein-Gordon equation

In order to introduce the quantum treatment of the relativistic electron scattering by the electromagnetic field, we will solve the Klein-Gordon equation. This approach

has the advantage of the simplicity over the Dirac equation, and we can expect to reproduce well the particle's behavior as long as the spin effects are not important. The Klein-Gordon equation for a charged particle of charge e and mass m in the presence of a single plane-wave electromagnetic field described by the four-vector potential $A(\phi)$ is

$$H(x)\psi(x) = 0, \qquad H(x) = -c^2\Pi_\mu\Pi^\mu + m^2c^4, \quad \Pi_\mu = \mathrm{i}\hbar\partial_\mu - eA_\mu(\phi), \tag{17}$$

where the Π_μ are the momentum operators. We emphasize here that in the case of a single plane wave electromagnetic field, both the Dirac and the Klein-Gordon equation are exactly solvable, the solutions being the so-called Volkov states [8, 9, 19]. In the case of a superposition of plane waves an approximate solution of the Klein-Gordon equation was given by Gavrila [16]; its method could be easily extended also for the Dirac equation.

Our approach is to solve the equation numerically; our starting point is the ansatz for the wave function proposed by Gavrila [16]: we look for the solution as the product of a plane wave and a function of the two variables $\phi_i = k_i \cdot x$, $i = 1, 2$:

$$\psi_{KG}(x) = \frac{1}{\sqrt{2E_p}} e^{\mathrm{i}p\cdot x} F(\phi_1, \phi_2). \tag{18}$$

In the absence of the field the solution reduces to a free plane wave of momentum p. The function $F(\phi_1, \phi_2)$ satisfies the equation [16]:

$$\begin{aligned} &D\frac{\partial^2 F(\phi_1,\phi_2)}{\partial\phi_1\partial\phi_2} + A_1\frac{\partial F(\phi_1,\phi_2)}{\partial\phi_1} + A_2\frac{\partial F(\phi_1,\phi_2)}{\partial\phi_2} + CF(\phi_1,\phi_2) = 0 \\ &D = -2\hbar k_1 \cdot \hbar k_2, \quad A_i = 2\mathrm{i}\hbar k_i \cdot (p - eA(\phi_i)), \\ &C = e^2A^2(\phi_1,\phi_2) - 2eA(\phi_1,\phi_2)\cdot p, \end{aligned} \tag{19}$$

If the particular gauge introduced in (7) is used, in the above equation the coefficients A_i reduce to constants $A_i = 2\mathrm{i}\hbar k_i \cdot p$ which simplifies considerably the numerical calculations. In order to solve the equation (19) numerically we need to define the domain of the variables ϕ_i and the boundary conditions. For the domain of each variable ϕ_i we consider the entire interval along which the corresponding field is non-zero, i.e. the interval defined in (5). The boundary conditions follow naturally by considering the equation at the edges of the interval. For example, if $\phi_1 = \phi_{m1}$ (at the lower boundary for ϕ_1) the field A_1 vanishes, and the problem reduces to the one of a particle in a single plane wave, for which the analytical solution is known to be the Volkov state [19]. Similarly, if $\phi_2 = \phi_{m2}$ (at the lower boundary for ϕ_2) the field A_2 vanishes, and the problem reduces to the Volkov problem for the first plane wave. Thus, the boundary conditions are

$$F(\phi_{m1}, \phi_2) = F_v(p; \phi_2), \quad F(\phi_1, \phi_{m2}) = F_v(p; \phi_1). \tag{20}$$

with $F_v(p;\phi_i)$ defined in Eq. (B9). The equation (19) with the previous boundary conditions is the so called Goursat problem [20], for which the standard numerical method is the ladder algorithm (see, for example [21]). With the notations introduced before and using the first order difference method for the derivatives, the equation can be written as

$$D\left(\frac{F_{i+1,j+1}-F_{i+1,j}-F_{i,j+1}+F_{i,j}}{\Delta\phi_1\Delta\phi_2}\right)+A_1\left(\frac{F_{i+1,j}-F_{i,j}}{\Delta\phi_1}\right)+ A_2\left(\frac{F_{i,j+1}-F_{i,j}}{\Delta\phi_2}\right)+C_{i,j}F_{i,j}=0. \quad (21)$$

from which we can obtain a recursive formula for the function $F_{i+1,j+1}$ in terms of the previous values $F_{i,j}, F_{i+1,j}, F_{i,j+1}$. This algorithm allows us to fill the domain of the variables ϕ_i and ϕ_2 starting from the corner (ϕ_{1m}, ϕ_{2m}). The main difficulty is that, in our problem, the typical value of the coefficient D is very small with respect to A_1 and A_2, which makes the calculation very unstable. For example, in the case of two plane waves of frequency 0.057 a.u., which corresponds to the wavelength $\lambda = 800$ nm, and for the case of an electron initially at rest, the ratio D/A_1 is of the order of 10^{-6}. To avoid this instability, an implicit scheme must be used; in our numerical calculations we employed an adapted version of the implicit scheme proposed by Gourlay [22].

3 Numerical results

We start by presenting the field used in the numerical calculation. We consider two plane waves, counter-propagating along the Oz axis and linearly polarized along the Ox axis; the envelopes are identical, consisting in Gaussian wings and a constant amplitude part of length 10λ. In all the calculations we take the frequency $\omega = 0.057$ a.u., which corresponds to the wavelength $\lambda = 800$ nm, and equal intensities which in the following will be characterized by the parameter ξ_0 defined in Eq. (4). In Fig. 1 we show the time dependence of the component A_x for a single plane wave (left panel) and the time average of A^2, as defined in Eq. (12), in the plane Oxz (right panel). The averaged A^2 depends only on z, as can be verified by simple calculations. We also notice that $\overline{A^2}$ is different from zero in a domain whose width is smaller than the duration of the field; in Fig. 1 (a) the flat portion of the plane wave is of 10λ, while the average $\overline{A^2}$ is non zero only in a domain of about 6λ. The explanation is that the fringe pattern in $\overline{A^2}$ is created by the interference of the two counter-propagating plane waves; the two waves are overlapping over a long time interval in the central part, but near the edges the duration of the overlap is smaller and the interference pattern is washed out.

Having established the field characteristics, we now turn to particle dynamics. Since the behavior of the particle in the presence of the field strongly depends on its initial position, we integrate the relativistic equations of motion (11) for a statistical ensemble of 50000 particles, initially at rest, distributed randomly within a disk of radius 5λ in the plane $y = 0$. In order to study the momentum transfer in its dependence on the particle's initial position, we represent, in the plane Oxy, each

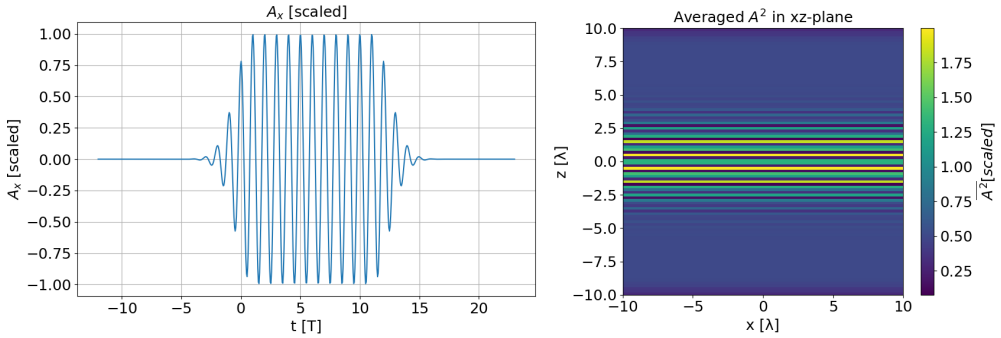

Figure 1 Left: The A_x component of the field for a single plane wave as a function of time (in arbitrary units). Right: The time average of A^2, as defined in Eq. (12), in the plane Oxz (in arbitrary units).

particle's initial position by a dot, whose color represents the final momentum, according to the color scale on the right side of the figure. In all cases, the momenta were scaled to the maximum momentum in the distribution, which is written in the title of each panel. Our calculations show that for this geometry the momentum transfer is mainly along the field propagation direction; this behavior is consistent with the prediction of the ponderomotive force approximation. Indeed, from Eq. (A4) we can see that since the dressed mass depends only on z, in the ponderomotive force approximation the force acting on the particle is along the z direction and the motion is one-dimensional. In Fig. 2 we show in the representation describe before the final momentum along the z axis for different values of the dimensionless intensity parameter $\xi_0 = 0.01, 0.05, 0.1, 0.5$. We notice that the momentum transfer increases with the intensity of the field. For the lowest value of ξ_0 the momentum map presents minima and maxima along the Oz axis, identical to the fringes in the averaged A^2; the bands in the map appear less intense for larger values of $|z|$, since the electrons whose initial position is at the edges of the disk, along the Oz direction do not experience the interaction with both fields simultaneously, but one at a time; by contrast, particles near the center of the disk interact with both fields simultaneously, and the momentum transfer is larger. For $\xi_0 = 0.05$ (Fig. 2 (b)) the bands in the momentum map are less regular in the central region, and for $\xi_0 = 0.1$ (Fig. 2 (c)) the regularity of the bands and the sharp margins between the bands are lost, which is an indication of the shift from the regular to the chaotic behavior [5]. The chaotic behavior is even more evident for $\xi = 0.5$ (Fig. 2 (d)); here we see bands with irregular margins and also the figure appears washed out because a few electrons acquire very large momenta, compressing the color scale for the others.

To conclude our analysis of the classical case, we discuss validity of the ponderomotive approximation. In Fig. 3 we present p_z as a function of time for $\xi_0 = 0.1$ (a) and $\xi_0 = 0.5$ (b). Although, as we mentioned, the actual trajectory is different for each particle in the statistical ensemble, the figure is representative for all the particles. We find very good agreement even at the largest ξ_0. In the figure we can clearly

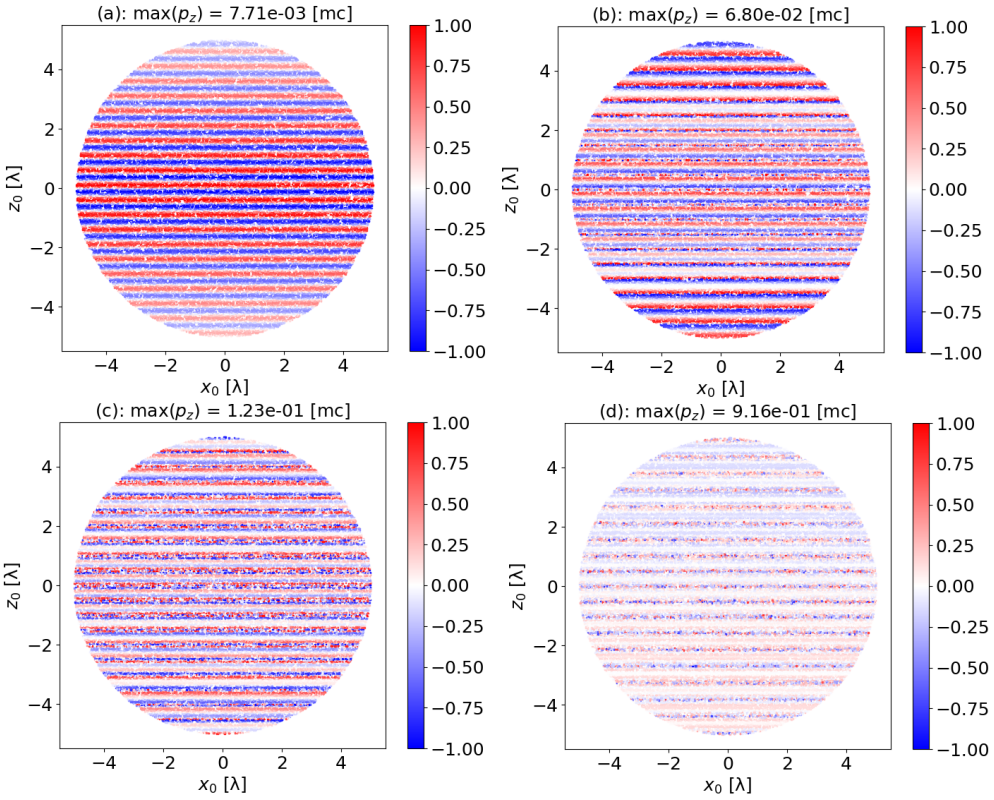

Figure 2 Final momentum distribution for a statistical ensemble of 50000 particles, initially at rest, distributed randomly within a disk of radius 5λ in the plane $y = 0$. (a): $\xi_{0=0.01}$. (b): $\xi_{0=0.05}$. (c): $\xi_{0=0.1}$, (d): $\xi_{0=0.5}$.

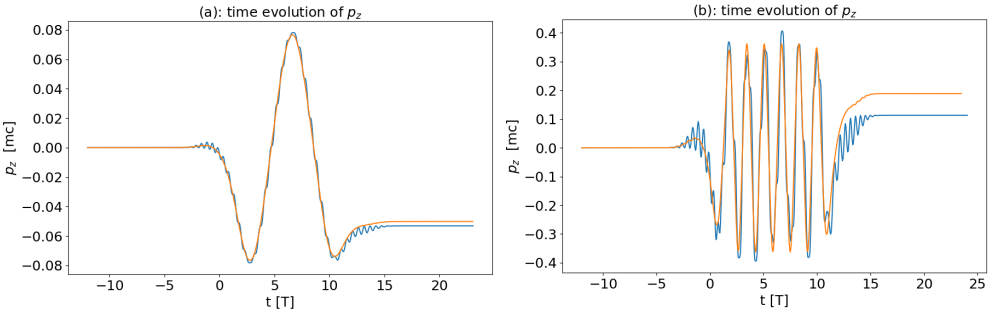

Figure 3 p_z as a function of the laboratory time t for $\xi_0 = 0.1$ (a) and $\xi_0 = 0.5$ (b).

see that the ponderomotive approximation smooths out the fast oscillations, but reproduces well the overall behavior of the particle. We emphasize here that, although

the integration of the equations of motion in the exact and the approximate case is done with respect to the proper time τ, the comparison must be done between the p_z of the exact and the approximate case, represented as function of the laboratory time t; the proper time will be different for the exact and approximate case, as the two trajectories are in fact very different (one fast oscillating and the other smooth).

In the remaining of this section we present the numerical results for the quantum case. For the dimensionless intensity parameter we chose as the initial value $\xi_0 = 0.01$. The geometry is head-on, and the two pulses considered were shorter than in the previous case, consisting only in the two wings, with no constant amplitude part. We calculated the function $F(\phi_1, \phi_2)$ for $p = (mc, 0, 0, 0)$ (a plane wave of zero momentum before the interaction with the field) according to the procedure described in the previous section. However for physical interpretation it is preferable to represent the function F in the coordinates $ct = (\phi_1 + \phi_2)/2$ and $z = (\phi_1 - \phi_2)/2$, as shown in the figure 4 (a), which presents the real part of F, and respectively (b) for the imaginary part.

At the initial moment, the wave function consists in two Volkov states, localized well apart from each other, created by the two plane waves. As the time progresses and the pulses overlap we can see the interaction near the central region of the two plots. Finally, after the pulses have crossed each other, the wave function has changed its shape and now it consists in two Volkov states, localized near the edges of the plots, plus a central part, non existent at the initial moment. This central part, where we can see an oscillatory behavior, is a clear indication of the momentum transfer along the field propagation direction, as we have seen also in the classical case. We mention here that the approximation presented in the paper by Gavrila [16] predict no net momentum transfer, which is in disagreement with our results. The comparison of the exact and the approximate results require further investigation, and we plan to address this topic in a future work.

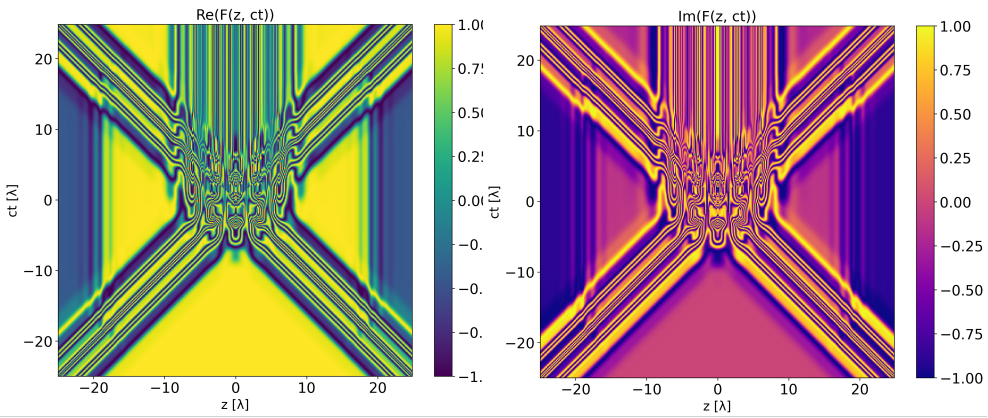

Figure 4 The real and the imaginary part of the function F defined in Eq. (18), represented in the plane (z, ct) for $\xi_0 = 0.05$ and $p = (mc, 0, 0, 0)$.

4 Conclusion

In conclusion, we studied in the classical and quantum formalism the scattering of relativistic electrons on a superposition of two counter-propagating linearly polarized plane waves.

In the classical case, since the particle trajectory strongly depends on its initial position, we calculated the trajectories for all the electrons in a statistical ensemble of 50000 particles and analyzed the results. We studied the distribution of the momentum transfer on the field parameters and the particle's initial position. We showed that the momentum transfer takes place mainly along the field propagation direction, and its magnitude increases with the intensity of the field. We also checked the validity of the ponderomotive force approximation, and we found that it agrees well with the exact results up to $\xi_0 \approx 0.5$.

In the quantum case, we studied the scattering of the particle on the field by solving the Klein-Gordon equation numerically; we compared the results with the classical predictions and with an analytical approximation. We found that, in the in the intensity domain considered, the quantum and classical results are in agreement at the qualitative level. Further investigation is required to compare them at the quantitative level.

Appendix A The relativistic equations of motion for a free particle of variable mass

Here we briefly present the relativistic Lagrangian formalism for a free particle of variable mass. Denoting by $\mathcal{M}(\mathbf{x}, t)$ the time and coordinate dependent mass, the covariant Lagrange function in the proper time parametrization is

$$L_{(\tau)} = -\mathcal{M}(x)c\sqrt{\frac{dx_\mu}{d\tau}\frac{dx^\mu}{d\tau}} = -\mathcal{M}(x)c\sqrt{\dot{x}_\mu \dot{x}^\mu} \tag{A1}$$

The Lagrange covariant equations of motion are obtained from

$$\frac{\partial L_{(\tau)}}{\partial x_\mu} = \frac{d}{d\tau}\frac{\partial L_{(\tau)}}{\partial \dot{x}_\mu} \tag{A2}$$

can be rewritten in the form

$$\frac{d}{d\tau}\left(\mathcal{M}(x)\dot{x}^\mu\right) = c^2\frac{\partial \mathcal{M}(x)}{\partial x_\mu}. \tag{A3}$$

A straightforward calculation yields the system of equations

$$\frac{dx^\mu}{d\tau} = u^\mu, \quad \frac{du^\mu}{d\tau} = \frac{1}{\mathcal{M}(x)}\left(c^2 g^{\mu\nu} - \dot{x}^\mu \dot{x}^\nu\right)\frac{\partial \mathcal{M}(x)}{\partial x^\nu}. \tag{A4}$$

The above system leads to results consistent with the condition

$$u \cdot u = c \text{ or } u \cdot \frac{du}{d\tau} = 0 \tag{A5}$$

as can be seen by noting that

$$u_\mu \frac{du^\mu}{d\tau} = \frac{1}{\mathcal{M}(x)} \left(c^2 g^{\mu\nu} - u^\mu u^\nu\right) u_\mu \frac{\partial \mathcal{M}(x)}{\partial x^\nu} = 0. \tag{A6}$$

Appendix B The Volkov solutions of the Klein-Gordon equation

In this appendix we briefly review the form and the main properties of the Volkov solutions of the Klein-Gordon equation; for a detailed presentation see, for example [19]. The Klein-Gordon Hamiltonian for a particle of charge e and mass m in the presence of a single plane-wave electromagnetic field described by the four-vector potential $A(\phi)$ is

$$H(x) = -c^2 \Pi_\mu \Pi^\mu + m^2 c^4, \quad \Pi_\mu = \mathrm{i}\hbar\partial_\mu - eA_\mu(\phi), \tag{B7}$$

and the Volkov solutions of the corresponding equation

$$H(x)\psi(x) = 0 \tag{B8}$$

are

$$\psi_\pm(p;x) = \frac{1}{\sqrt{2E_p}} e^{\mp \frac{\mathrm{i}}{\hbar} p\cdot x} F_v(p;\phi), F_v(p;\phi) = e^{\pm \frac{\mathrm{i}}{2\hbar(k\cdot p)} \int_{\phi_0}^{\phi} \mathrm{d}\chi \left(e^2 A^2(\chi) \mp 2eA(\chi)\cdot p\right)} \tag{B9}$$

The $\pm$ sign denotes the positive and negative frequency solutions, respectively, and k is the four-wave vector of the electromagnetic field. In the limit $A \to 0$ the Volkov solutions reduce to plane waves of momentum p.

The Volkov solutions are orthogonal with respect to the Klein-Gordon scalar product in the presence of the electromagnetic field

$$\begin{aligned} \langle f(x), g(x)\rangle_{KG-f} &= \int \mathrm{d}\mathbf{r} f^*(x) \left[\mathrm{i}\hbar \overset{\leftrightarrow}{\partial}_0 - 2ceA_0(\phi)\right] g(x) \\ &\equiv \int \mathrm{d}\mathbf{r} \left[f^*(x)\mathrm{i}\hbar \frac{\partial g(x)}{\partial t} - g(x)\mathrm{i}\hbar \frac{\partial f^*(x)}{\partial t} - 2ceA_0(\phi) f^*(x) g(x)\right], \end{aligned} \tag{B10}$$

obeying the relations

$$\langle \psi_{\pm}(p_1;x), \psi_{\pm}(p_2;x) \rangle_{KG-f} = \pm\delta(\mathbf{p}_1 - \mathbf{p}_2), \quad \langle \psi_{\pm}(p_1;x), \psi_{\mp}(p_2;x) \rangle_{KG-f} = 0. \tag{B11}$$

The KG Volkov states also form a complete set. The completeness property for the solutions of the KG equation in the presence of the field can be expressed as the pair of relations

$$\begin{aligned} &\int \mathrm{d}\mathbf{p} \left[\psi_+(p;x) \left(\mathrm{i}\hbar \frac{\partial \psi_+(p;x')}{\partial t} \right)^* - \psi_-(p;x) \left(\mathrm{i}\hbar \frac{\partial \psi_-(p;x')}{\partial t} \right)^* \right] = \delta(\mathbf{x} - \mathbf{x}'), \\ &\int \mathrm{d}\mathbf{p} \left[\psi_+(p;x)\psi_+^*(p;x') - \psi_-(p;x)\psi_-^*(p;x') \right] = 0. \end{aligned} \tag{B12}$$

References

[1] Salamin, Y.I., Faisal, F.H.M.: Ponderomotive scattering of electrons in intense laser fields. Phys. Rev. A **55**(5), 3678–3683 (1997) https://doi.org/10.1103/PhysRevA.55.3678

[2] Startsev, E.A., McKinstrie, C.J.: Multiple scale derivation of the relativistic ponderomotive force. Phys. Rev. E **55**(6), 7527–7535 (1997) https://doi.org/10.1103/PhysRevE.55.7527

[3] Dodin, I.Y., Fisch, N.J., Fraiman, G.M.: Drift Lagrangian for a relativistic particle in an intense laser field. Jetp Lett. **78**(4), 202–206 (2003) https://doi.org/10.1134/1.1622032

[4] Axelrod, J.J., Campbell, S.L., Schwartz, O., Turnbaugh, C., Glaeser, R.M., Müller, H.: Observation of the Relativistic Reversal of the Ponderomotive Potential. Phys. Rev. Lett. **124**(17), 174801 (2020) https://doi.org/10.1103/PhysRevLett.124.174801

[5] Bauer, D., Mulser, P., Steeb, W.-H.: Relativistic Ponderomotive Force, Uphill Acceleration, and Transition to Chaos. Phys. Rev. Lett. **75**(25), 4622–4625 (1995) https://doi.org/10.1103/PhysRevLett.75.4622

[6] Sarachik, E.S., Schappert, G.T.: Classical Theory of the Scattering of Intense Laser Radiation by Free Electrons. Phys. Rev. D **1**(10), 2738–2753 (1970) https://doi.org/10.1103/PhysRevD.1.2738

[7] Gordon, W.: Der Comptoneffekt nach der Schrodingerschen Theorie. Z. Physik **40**(1-2), 117–133 (1926) https://doi.org/10.1007/BF01390840

[8] Wolkow, D.M.: Uber eine Klasse von Losungen der Diracschen Gleichung. Z. Physik **94**(3-4), 250–260 (1935) https://doi.org/10.1007/BF01331022

[9] Bagrov, V.G., Gitman, D.: The Dirac Equation and Its Solutions. De Gruyter Studies in Mathematical Physics, vol. 4. De Gruyter, Berlin (2014). https://doi.org/10.1515/9783110263299

[10] Kapitza, P.L., Dirac, P.A.M.: The reflection of electrons from standing light waves. Math. Proc. Camb. Phil. Soc. **29**(2), 297–300 (1933) https://doi.org/10.1017/S0305004100011105

[11] Rosenberg, L.: Effect of virtual Compton scattering on electron propagation in a laser field. Phys. Rev. A **49**(2), 1122–1130 (1994) https://doi.org/10.1103/PhysRevA.49.1122

[12] Li, X., Zhang, J., Xu, Z., Fu, P., Guo, D.-S., Freeman, R.R.: Theory of the Kapitza-Dirac Diffraction Effect. Phys. Rev. Lett. **92**(23), 233603 (2004) https://doi.org/10.1103/PhysRevLett.92.233603

[13] Hebenstreit, F., Alkofer, R., Dunne, G.V., Gies, H.: Momentum signatures for Schwinger pair production in short laser pulses with a subcycle structure. Phys. Rev. Lett. **102**, 150404 (2009) https://doi.org/10.1103/PhysRevLett.102.150404

[14] Salamin, Y.I., Hu, S.X., Hatsagortsyan, K.Z., Keitel, C.H.: Relativistic high-power laser–matter interactions. Physics Reports **427**(2-3), 41–155 (2006) https://doi.org/10.1016/j.physrep.2006.01.002

[15] Di Piazza, A., Hatsagortsyan, K.Z., Keitel, C.H.: Quantum radiation reaction effects in multiphoton Compton scattering. Phys. Rev. Lett. **105**, 220403 (2010) https://doi.org/10.1103/PhysRevLett.105.220403

[16] Gavrila, M.: Crossed-laser-beam solutions for the Klein-Gordon equation. Phys. Rev. A **99**(1), 012120 (2019) https://doi.org/10.1103/PhysRevA.99.012120

[17] Northrop, T.G.: The Adiabatic Motion of Charged Particles. Interscience Tracts on Physics and Astronomy, vol. 21 (1963)

[18] Brown, L.S., Kibble, T.W.B.: Interaction of Intense Laser Beams with Electrons. Phys. Rev. **133**(3A), 705–719 (1964) https://doi.org/10.1103/PhysRev.133.A705

[19] Boca, M.: On the properties of the Volkov solutions of the Klein–Gordon equation. J. Phys. A: Math. Theor. **44**(44), 445303 (2011) https://doi.org/10.1088/1751-8113/44/44/445303

[20] Goursat, E.: A Course in Mathematical Analysis. Dover Publications, New York (1959)

[21] Ames, W.F.: Numerical Methods for Partial Differential Equations, 2d ed edn. Computer science and applied mathematics. Academic Press, New York (1977)

[22] Gourlay, A.R.: A note on trapezoidal methods for the solution of initial

value problems. Math. Comp. **24**(111), 629–633 (1970) https://doi.org/10.1090/S0025-5718-1970-0275680-3